Spring 2015

High density collagen fibril constructs with tunable mechano-biology in acellular and cellular configurations

Kevin Blum
Purdue University

PURDUE UNIVERSITY
GRADUATE SCHOOL
Thesis/Dissertation Acceptance

This is to certify that the thesis/dissertation prepared

By Kevin Blum

Entitled
HIGH DENSITY COLLAGEN FIBRIL CONSTRUCTS WITH TUNABLE MECHANO-BIOLOGY IN ACELLULAR AND CELLULAR CONFIGURATIONS

For the degree of Master of Science in Biomedical Engineering

Is approved by the final examining committee:

Sherry Voytik-Harbin
Chair

Corey Neu

Stacey Halum

To the best of my knowledge and as understood by the student in the Thesis/Dissertation Agreement, Publication Delay, and Certification Disclaimer (Graduate School Form 32), this thesis/dissertation adheres to the provisions of Purdue University's "Policy of Integrity in Research" and the use of copyright material.

Approved by Major Professor(s): Sherry Voytik-Harbin

Approved by: George R. Wodicka 4/13/2015
Head of the Departmental Graduate Program Date

HIGH DENSITY COLLAGEN FIBRIL CONSTRUCTS WITH TUNABLE MECHANO-BIOLOGY IN ACELLULAR AND CELLULAR CONFIGURATIONS

A Thesis

Submitted to the Faculty

of

Purdue University

by

Kevin M Blum

In Partial Fulfillment of the

Requirements for the Degree

of

Master of Science in Biomedical Engineering

May 2015

Purdue University

West Lafayette, Indiana

For my family, friends, lab mates, and particularly Angela for helping and putting up with me throughout it all. Thank you.

ACKNOWLEDGMENTS

This work was funded in part by the Purdue University Office of the Vice President for Research Incentive Grant Funds, the Purdue University Charles C. Chappelle Fellowship, and the NSF Graduate Research Fellowship Program under Grant No. DGE-0833366 (TN).

TABLE OF CONTENTS

Page

LIST OF TABLES

LIST OF FIGURES

ABSTRACT

Blum, Kevin M. M.S.B.M.E., Purdue University, May 2015. High Density Collagen Fibril Constructs With Tunable Mechano-Biology in Acellular and Cellular Configurations. Major Professor: Sherry Voytik-Harbin.

Collagen has long been used as a material for tissue engineering due to its prevalence in the extracellular matrix of connective tissues. However, traditional collagen materials utilizing atelocollagen and acid solubilized telocollagen have lacked the mechanical integrity and collagen fibril density found in the in vivo state. Here, we utilize collagen oligomers and confined compression to forcibly remove a portion of the fluid phase component. Materials were created with controlled, substantially increased material properties, including order of magnitude increases in collagen fibril density, elastic modulus, compressive modulus,and resistance to proteolytic degradation. The technique was found to be amenable to cell encapslation, allowing the creation of viable cellularized high density constructs. The translational aspects of these high density collagen materials was examined through the ultrastructure and bulk property changes that may be present through lyophilization and rehydration, as well as comparison against a gold standard market crosslinked microfibrillar collagen sponge.

CHAPTER 1. INTRODUCTION

1.1 Introduction

In vivo, cells reside within a tissue specific extracellular matrix (ECM), made up of a mixture of proteins, primarily Type I collagen. In vivo, collagen exhibits ordering over several length scales, including molecular (10^{-9} m), fibrillar (10^{-6} m), suprafibrillar (10^{-3} m), and tissue/organ (10^{-1} m). The chemical and physical properties of this matrix guide cellular proliferation, migration, and differentiation[1]. Because of this, tissue engineering as a field seeks to recapitulate the design features of the natural ECM. Because Type I collagen makes up around 90% of the ECM, and is highly conserved across tissues and species, it is a logical choice for a tissue engineering material[2, 3] However, to date, there has been a lack of a tunable collagen material with physiologically relevant properties and signaling capabilities, limiting collagen's use in both research and clinical settings.

Soluble monomeric collagens, atelocollagen and telocollagen, are commonly used in the research setting, and are characterized by the absence of the natural intermolecular crosslinks found in in vivo collagen[4]. This protein structure results in the collagen molecules, upon polymerization, self-organizing into long, randomly oriented fibrils[5]. This microstructure is characterized by its low mechanical integrity and rapid proteolytic degradation[6]. Monomeric collagen formulations have historically been limited by

solubility to low collagen fibril densities (<10 mg/mL), further limiting their mechanical integrity, tunability, and physiological relevance[7].

Because of the inherent mechanical weakness present in monomeric collagen formulations, several techniques have been developed to increase the collagen density and/or mechanical integrity, and are discussed in detail in Chapter 2. Crosslinking of collagen attempts to increase the mechanical integrity and resistance to proteolytic degradation through physical means, such as dehydrothermal treatment, or chemical means, such as nonspecific glutaraldehyde crosslinking. These techniques increase the mechanical integrity of the collagen material, but have the drawbacks of destruction of the microstructure and blocking of the inherent biological signaling capabilities of the collagen. Increasing the collagen density is typically accomplished through centrifugation or microinjection with continuous evaporation[8, 9]. These methods are relatively time consuming, and, although they allow for cellular migration across them, they typically are not amenable to cell encapsulation or infiltration[10]. More recently, removal of the fluid phase of polymerized telocollagen has been shown to greatly increase the mechanical integrity and fibril density of the matrix, but the process requires the removal of nearly the entire fluid phase of the matrix, and resulting materials are very thin (<100 um thick) and brittle[11, 12].

In order to overcome the issues with monomeric collagens, decellularized tissues or fibrillary collagen sponges may be used, and are discussed in Chapter 3. Decellularized tissues contain the assortment of proteins found in the natural extracellular matrix outside of collagen, but are subject to the inherent variability of their source tissues[3, 13]. Fibrillar collagen sponges are created through lyophilization of slurries of

insoluble collagen particulate, and are characterized by their amorphous microstructure of densely packed fibrils separated by large pores hundreds of microns across[14]. These sponges are often exogenously crosslinked to create the collagen hemostats and drug carriers current on the market for clinical use[15].

To date there remains an inability to create high-density fibril materials that recreate hierarchical assembly of collagen found in mature tissues and tunable cell-instructive capacity. This research works to overcome this technology gap using a hierarchical design strategy focused on molecular level building blocks specified based on intermolecular crosslink composition and polymerization capacity. To this end, the Voytik-Harbin lab has developed a method to extract and purify a new collagen building block, termed collagen oligomer, which represents a new soluble subdomain that falls between molecular and fibrillar size scales[5, 16]. Oligomers represent aggregates of tropocollagen molecules (e.g., trimer) that retain their natural intermolecular crosslink[17]. When polymerized, collagen oligomers exhibit suprafibrillar assembly forming interconnected fibril network and demonstrating mechanical integrity far exceeding that of conventional monomer collagen formulations[6]. Previous work has documented that modulation of polymerization parameters including total collagen concentration and oligomer to monomer ratio can be used as an effective means to control fibril level properties, including microstructure, mechanical properties (e.g. stiffness), and proteolytic degradation, which are all known to guide cell fate[18-20]. However, oligomer collagen solutions are still limited to 10 mg/mL by the same solubility constraints that affect monomer collagen solutions, limiting their potential to create high fibril-density collagen matrices. To overcome this limitation, a confined compression approach was

used in this work to forcibly remove a portion of the interstitial fluid low-density oligomer matrices, effectively creating high collagen-fibril density materials with tunable material properties.

The specific aims of this research were as follows:

1. Develop and validate the utility of confined compression as a scalable method for creating tunable high-density collagen-fibril materials and engineered tissue constructs;
2. Define how lyophilization and rehydration effects the multi-scale structure, mechanical properties, and proteolytic degradation of high-density collagen-fibril materials; and
3. Compare ultrastructure, mechanical properties, and proteolytic degradation of high-density collagen-fibril materials to the commercial collagen sponge Helistat

Chapter 2 of this thesis addresses Specific Aim 1, while efforts related to Specific Aim 2 and 3 are descried in Chapter 3. Finally, overall conclusions of the work as well as opportunities for future studies are addressed in Chapter 4.

Results from this work are important because they support the rational, translational, and scalable design of a broad range of collagen-based materials and cell-encapsulated tissue constructs with tissue-like fibril densities, suprafibrillar organizations, and functional properties for tissue engineering and regenerative medicine applications.

CHAPTER 2. ACELLULAR AND CELLULAR HIGH-DENSITY, COLLAGEN-FIBRIL CONSTRUCTS WITH SUPRAFIBRILLAR ORGANIZATION

2.1 Background

In vivo, connective tissue cells reside within a tissue-specific extracellular matrix (ECM) which primarily represents a highly organized network of densely packed fibrous proteins, primarily type I collagen fibrils. It is well established that the suprafibrillar organization and architecture of the collagen contributes to the diversity of structural and functional properties displayed by the various tissues of the body[1]. However, more recently, the microstructure, mechanical properties (e.g., stiffness), and proteolytic degradation properties of this fibril network have been recognized as powerful morphogens along with the more widely studied soluble factor and cell-cell signaling[21]. Here, type I collagen fibrils instruct fundamental cellular behaviors (e.g., proliferation, differentiation, migration, and matrix remodeling) associated with tissue development, maintenance, and repair through their inherent molecular signaling domains, including those involved in cell adhesion, growth factor binding, and collagen proteolytic degradation, as well as structural constraints[22]. As such, it is not surprising that a major goal of tissue engineering and regenerative medicine is the functional design of biomaterials and tissues that replicate these essential multi-scale biochemical and mechanobiology features.

As the major structural protein of tissues, type I collagen demonstrates not only hierarchical, multi-scale organization but also the capacity to self-assemble into fibrous tissues in vivo. As shown in Figure 1, the organizational levels of collagenous tissues span various size scales including molecular (10^{-9} m), fibrillar (10^{-6} m), suprafibrillar (10^{-3} m), and tissue/organ (10^{-1} m), with tropocollagen (also known as telocollagen) representing the fundamental collagen polymer building block. Tropocollagen molecules, which comprise a central triple helical region flanked by short non-helical telopeptide domains, participate in a nucleation and growth mechanism to yield microfibrils which in turn associate laterally and axially to yield fibrils. Proper molecular alignment is driven by hydrophobic and electrostatic interactions[23, 24] with additional adjustments likely provided by enzyme-mediated molecular crosslinking which further stabilize the molecular and fibril assemblies[25, 26]. Although extensive in-vitro study has provided a detailed mechanistic understanding of the molecular assembly of individual collagen fibrils (termed fibrillogenesis or fibrillar assembly)[24], much less is known regarding processes associated with suprafibrillar assembly and higher-order organization[25]. This knowledge gap has hindered the rational design and development of collagen-fibril materials and tissue constructs with complex hierarchical architectures and biophysical and cell-instructive properties found in mature tissues.

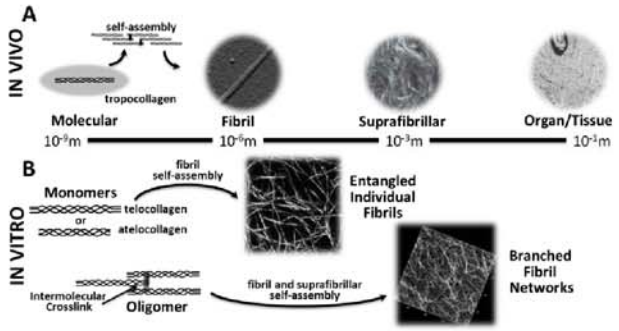

Figure 1 - Hierarchical, multi-scale organization of type I collagen as occurs in vivo (A) and in-vitro with polymerizable monomer (atelocollagen and telocollagen) and oligomer formulations (B).

To date, collagen-based material and tissue design for both research and medical applications has relied on a limited number of collagen formulations known to vary in purity, solubility, and in-vitro polymerization (self-assembly) capacity[27] . In vitro fibril assembly of collagen molecules occurs spontaneously at physiologic pH and ionic strength. However, self-assembly kinetics and fibril morphology are highly dependent upon the collagen molecule integrity (presence or absence of telopeptide regions), extraction methods, and self-assembly conditions including buffer composition, temperature, and presence of accessory molecules (e.g., other collagen types)[1, 10, 23, 24, 28]

Conventional soluble monomer formulations, namely telocollagen and atelocollagen, exhibit fibril self-assembly and are commonly used to create low-density, collagen-fibril matrices for 3D cell culture and tissue engineering applications. These matrices are typically prepared at collagen concentrations of 20 mg/mL or less, largely owing to the limited molecular solubility and/or high viscosity of collagen solutions [4, 29]. Because of their inability to induce supramolecular assembly and higher order interfibril associations, monomers yield matrices that represent entanglements of long individual

fibrils[17]. Therefore, even at high densities (10-20 mg/ml), these matrices are associated with poor shape definition, low mechanical integrity, poor handling, cell-induced contraction, and rapid proteolytic degradation[6, 30-32].

More recently, methods have been described for creating high-density collagen-fibril materials from soluble collagen formulations that better approximate the structural hierarchy and mechanical properties of mature tissues, as seen in Table 1. These methods, which include reverse dialysis, ultracentrifugation, and evaporation, involve generating high concentrations of acid-soluble collagen monomers (>20 mg/ml) followed by neutralization to induce fibrillogenesis. The majority of these approaches were inspired by current theories and evidence that collagen suprafibrillar organization often mimic geometries described in liquid crystalline states[5]. For example, reverse dialysis of low concentration monomer solutions against poly(ethylene glycol) (PEG)[8, 9, 27] has been used alone or in conjunction with continuous microchamber injection to yield high-density matrices that are homogenous (250 mg/ml) or display gradients (50-500 mg/ml)[33] . A similar approach involving microinjection and evaporation followed by fibrillogenesis yielded concentration and ultrastructure gradients extending from 5-1000 mg/ml[10]. Unfortunately, these approaches require long production times (weeks to months) and are not amenable to cell encapsulation. Furthermore, while these high density materials support cell adhesion and growth along the surface, migration or infiltration into the material is limited[34, 35].

Table 1 – Densification Strategies

Process	Neutralization	Final Formulation	Mechanical Properties	Cell Encapsulation	Ref
centrifugation prior to polymerization; 90 min	PBS	10-20 mg/mL constructs	up to 70kPa elastic modulus	yes	Puetzer, 2013. Elsdale, 1972.
continuous injection/ evaporation; weeks to months	ammonia vapor	thin matrices up to 1000 mg/mL	not shown	no	Mosser, 2006. Besseau, 1995.
reverse dialysis with PEG prior to polymerization; 24 hours	Titration of PEG	375 mg/mL	not shown	No	Saeidi, 2012. Knight 1998.
post polymerization unconfined compression/ absorbtion; 5 min	DMEM and NaOH	dense thin sheets (~98% weight loss)	up to 4 Mpa elastic modulus	yes, but cell death under extreme compressive conditions	Neel, 2006. Bitar, 2007. Cheema, 2013. Mudera, 2007. Brown, 2005. Hadjipanayi, 2009.

An alternative 2-step method for achieving high-density collagen-fibril materials that is more amenable to cell encapsulation involves polymerization of low concentration monomer solutions followed by unconfined plastic compression and/or capillary fluid flow into blotting paper layers to reduce the interstitial fluid content [11]. Here, low-loads (50-60 g or 1.1 kPa) are applied to the top of a collagen matrix (~ 2-5 mg/ml) to achieve fluid reduction (~85-99.8% compressive strain) through a supporting nylon mesh[11, 36]. The resulting sheets, which are 20 to 100 um in thickness, are fragile, requiring spiraling

to facilitate handling and further testing. They display tensile strength and modulus values of 0.6 ± 0.11 MPa and 1.5 ± 0.36 MPa, respectively, and support 85% viability of encapsulated cells[12]. Additional compression of spiraled constructs improves mechanical integrity but reduces cellular viability[12, 36].

In the present work, we demonstrate the benefit of combining suprafibrillar assembly with fibril-matrix densification strategies for creating broadly customizable, scalable, high-density collagen-fibril constructs in the presence and absence of cells. The first step involves the use of standardized collagen oligomers to prepare low concentration matrices (<10 mg/ml) with specified and highly reproducible microstructure and physical properties (intermolecular crosslink content, fibril density, interfibril branches, and proteolytic degradability). Oligomers, which represent soluble aggregates of tropocollagen molecules (e.g., trimers) that retain their natural intermolecular crosslinks, exhibit not only fibrillar but also suprafibrillar assembly. Next, confined, rather than unconfined, compression is applied to controllably reduce fluid content and increase the fibril density. Interestingly, we show that this approach is not applicable to collagen-fibril matrices prepared from conventional collagen monomer preparations, telocollagen and atelocollagen. This is largely owing to their limited self-assembly capacity and inability to yield fibril microstructures that can sustain or support the associated compressive and fluid shear forces. Results from this work are important because they support the rational and scalable design of a broad range of collagen-based materials and cell-encapsulated tissue constructs with tissue-like fibril densities, suprafibrillar organizations, and functional properties for tissue engineering and regenerative medicine applications.

2.2 Materials and Methods

2.2.1 High-Density Collagen-Fibril Construct Preparation

Type I collagen oligomers were acid solubilized from dermis of market weight pigs and lyophilized for storage as described previously[18]. Prior to use, the lyophilized collagen was dissolved in 0.01 N hydrochloric acid (HCl) and rendered aseptic by chloroform exposure at 4°C. Collagen concentration was determined using a Sirius Red (Direct Red 80) assay[37]. The oligomer formulation was standardized based upon purity as well as polymerization capacity according to ASTM standard F3089-14[38]. Here, polymerization capacity is defined by matrix shear storage modulus (G') as a function of collagen concentration of the polymerization reaction. Commercial acid-soluble rat tail collagen (telocollagen) and pepsin-solubilized bovine dermis collagen (atelocollagen) were obtained from Corning (Corning, NY) and Advanced BioMatrix (Carlsbad, CA), respectively. All collagen solutions were diluted with 0.01 N HCl to achieve desired concentrations and neutralized with 10X phosphate buffered saline (PBS) and 0.1N sodium hydroxide (NaOH) to achieve pH 7.4[17]. Neutralized solutions were kept on ice prior to inducing polymerization by warming to 37°C.

All acellular oligomer collagen-fibril constructs were prepared with an initial starting collagen concentration of 3.5 mg/ml in 2 cm X 4 cm block molds. After polymerization and incubation at 37°C for 1 hour (tensile testing only) or 18 hours (used for all tests), each construct was compressed within the block mold to a final thickness of 2 mm (1.6 mL volume) with a porous polyethylene platen (50 μm pore size; Scientific Commodities, Inc., Lake Havasu City, AZ) at a rate of 6 mm/min. Final construct

collagen concentration was controlled by varying the initial polymerized collagen volume. More specifically, starting volumes of 1.6 mL, 5.6 mL, and 11.2 mL of 3.5 mg/mL collagen (initial concentration) were differentially compressed to yield 3.5 mg/ml (no compression), 12.25 mg/ml (71% strain), and 24.5 mg/mL (86% strain) constructs, respectively. Assuming all collagen polymerized, these constructs represented collagen wet weights (w/w) of 0.6%, 2.1% and 4.2%, respectively, as measured from the masses of hydrated and lyophilized constructs (data not shown). Commercial telocollagen and atelocollagen were polymerized to a collagen concentration of 3.5 mg/mL and allowed to polymerize at 37C for 18 hours before being subjected to compression identical to that detailed above to 86% strain.

2.2.2 Collagen Fibril Micro- and Ultra-Structure Analysis

The fibril microstructure and ultrastructure of the collagen constructs was visualized using confocal reflection microscopy[39] and cryo-SEM[40], respectively. Confocal reflection microscopy was performed using an Olympus Fluoview FV-1000 confocal system adapted to an Olympus IX81 invested microscope with a 60X UPlanSApo water immersion objective (Olympus, Tokyo, Japan). Cryo-SEM images of samples were obtained using an FEI NOVA nanoSEM 200 (FEI, Hillsboro, OR). Samples were quick frozen by submersion into liquid nitrogen cooled to its triple point, transferred to a CT1000 coldstage attachment (Oxford Instruments North America, Inc., Concord, MA), and sublimated under vacuum before sputter coating and imaging.

Collagen constructs used for AFM analysis of D-periodic banding were extensively rinsed with water and then air dried. Samples were imaged in air using a

Bruker BioScope Catalyst AFM (Bruker Corporation, Santa Barbara, CA) as described previously[41]. In brief, images were acquired in a peak force tapping mode using ScanAsyst Fluid+ probes (silicon tip, silicon nitride cantilever, nominal tip radius 2 nm and nominal stiffness of 0.7 N/m). From each sample (n=4 per group), 15-20 fibrils at each of 2 locations were imaged and analyzed (~150 total fibrils per group). Two-dimensional fast fourier transforms were performed and the primary peak from the 2D power spectrum was analyzed to determine the value of the D-periodic spacing for individual fibrils.

2.2.3 Mechanical Testing

Tensile testing was performed on dog-bone shaped collagen constructs with a gauge length, width, and thickness of 26 mm, 4 mm, and 2 mm, respectively. All samples were tested in uniaxial tension to failure at a strain rate of 10 mm/second using a servo electric materials testing system (Testresources, Shakopee, MN). Stress measurements were obtained using a 10 lb load cell (LPM 512, Cooper Instruments, Warrenton, VA) at a sampling rate of 100 Hz. Engineering tensile modulus (E_T) was calculated from the linear region of the stress strain curve. Ultimate stress ($\boldsymbol{\sigma}_U$) represented peak stress experienced by the sample, and failure strain (ε_f) was the strain at which constructs experienced total failure. (n=7).

2.2.4 Proteolytic Degradability

Proteolytic degradation was measured by measuring compressive modulus and hydroxyproline content of constructs before and after 2-hour exposure to bacterial collagenase type IV (31.2 U/mL; Worthington, Lakewood, NJ). Collagen constructs

prepared at 3.5, 12.25, and 24.5 mg/mL were punched to form cylinders with diameter and thickness of 1 cm and 2 mm, respectively. Constructs were tested in unconfined compression at 17%/second to 75% strain using a servo electric materials testing system (Testresources, Shakopee, MN) adapted with a 10 lb load cell (LPM 512, Cooper Instruments, Warrenton, VA). Compressive modulus was calculated as the slope of the linear region of the stress-strain curve. Compression tests were performed on seven independent constructs per group (n=7). Control and collagenase-treated constructs were then subjected to a spectrophotometric-based hydroxyproline assay (Sigma Aldrich) to determine collagen content.

2.2.5 Cellularized High-Density Tissue Construct Preparation

Low passage human adipose-derived stem cells (hASC) were obtained from Zen-Bio (Research Triangle Park, NC). Cells were cultured in 50/50 mixture of DMEM/F12 medium (Life Technologies, Carlsbad, CA) with 10% FBS, 100 U/mL Penicillin, and 100 U/mL Streptomyosin (Invitrogen, Grand Island, NY). hASC were grown and maintained in a humidified environment of 5% carbon dioxide in air at 37°C. Cells were kept below 80% confluence and used in experiments at passage 6 to 9.

To create cellularized, high-density, collagen-fibril constructs, hASC were added to neutralized oligomer solutions (3.5 mg/mL) and polymerized for 15 minutes at 37°C (Figure 7). Tissue constructs representing different volumes, specifically 50 µL, 175 µL, or 350 µL, were created in glass-bottom 96-well plate (Corning, Corning, NY). Constructs were densified to 1.5 mm final thickness (50 µL volume) at 6 mm/min using a porous polyethylene platen (Scientific Commodities, Inc.). Final hASC density within

constructs was 5 x 10^5 cells/mL. Immediately following densification, 200 µL of medium was added to each well and tissue constructs were maintained in a humidified environment at 37^{o}C and 5% CO_2 in air with medium changes every 24 hours.

Cell viability was evaluated at 48 hours by staining with Celltracker (5-chloromethylfluorescein diacetate; Molecular Probes, Eugene, OR) and propidium iodide (Sigma-Aldrich). Confocal images stacks (50-µm thick) were collected and used for live/dead analyses (n=6). Cell morphology and cell-matrix interactions were assessed by staining constructs with phalloidin (Molecular Probes, Eugene, OR) and Draq5 (Biostatus Limited, Leicestershire, United Kingdom) for visualization of F-actin and the nucleus, respectively.

2.2.6 Statistical Analysis

Statistical analysis was performed in Minitab statistical software. One-way ANOVA was applied across collagen concentrations (3.5, 12.25, and 14.5 mg/mL) with a Tukey post-hoc test to determine differences in mean values. In cases where population variances were not equal (ultimate stress, elastic modulus, compressive modulus), a Kruskal-Wallis test was performed in place of ANOVA with post-hoc 2-sample T-tests assuming non-equal population variances. Mean D-periodic spacing values were compared using an ANOVA and a post-hoc Holm-Sidak test. To examine differences in the distribution of fibril D-periodic spacing values, the Cumulative Distribution Function (CDF) of each group was computed and statistically compared using a Kolmogorov-Smirnov (KS) test. A critical global p-value of 0.05 was used.

2.3 Results and Discussion

2.3.1 Type I Collagen Oligomers Demonstrate in-vitro Fibrillar and Suprafibrillar Assembly and Support Confined Compression

Recently, we described the isolation and purification of type I collagen oligomers, which appear to represent a new soluble subdomain that falls between molecular and fibrillar size scales[16, 17]. As shown in Figure 1B, oligomers represent tissue-derived aggregates of tropocollagen molecules (e.g., trimer) that retain their natural intermolecular crosslink. Unlike conventional collagen monomers, oligomers exhibit rapid fibril and suprafibrillar self-assembly yielding highly interconnected collagen-fibril matrices with dramatically improved mechanical integrity, handling, and reduced proteolytic degradation[6]. As a result when polymerized at the same final collagen concentration, oligomer matrices have dramatically improved shape retaining capacity, mechanical integrity, and resistance to cell-induced contraction compared to their monomer counterparts[5]. More specifically, the stiffness range prepared for oligomer matrices prepared at 0.5-4 mg/ml was 40-1500Pa, while that for telocollagen and atelocollagen preparations was 2-300Pa and 2-50Pa, respectively[6].

Here, high resolution AFM images (Figure 2) were used to confirm that low-density oligomer matrices represent highly interconnected fibril networks with D-periodic spacing resembling that found in vivo. As shown in Figure 2A-C, component fibrils within oligomer and telocollagen but not atelocollagen matrices displayed highly regular and prominent D-periodic spacing patterns. These results confirm previous studies demonstrating the essential role of the non-helical telopeptide regions in guiding

the correct periodic assemblies and crosslinking of fibrils[42, 43]. Further quantitative analysis revealed that mean fibril D-periodic spacing for telocollagen and oligomer matrices were statistically similar (p=0.299), with values of 66.1 ± 0.1 nm (n=4; 164 fibrils) and 66.7 ± 0.9 nm (n=4; 144 fibrils), respectively. However, evaluation of the D-spacing distribution, when plotted in histogram (Figure 2D) or cumulative distribution (Figure 2E) formats, showed a statistically significant (p<0.001) rightward shift toward higher values for oligomer compared to telocollagen. These results further support the notion that oligomers with their inherent intermolecular crosslinks assist in establishing the precise ordering and alignment during self-assembly[26].

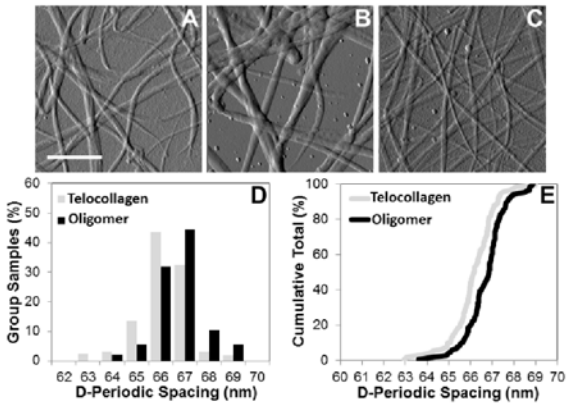

Figure 2 - Qualitiative and quantitative determination of D-periodic spacing for polymerized matrices (0.5 mg/ml). Representative AFM error image show prominent D-periodic spacing patterns for (A) Oligomer and (B) Monomer but not (C) Atelocollagen. (D) Histogram p

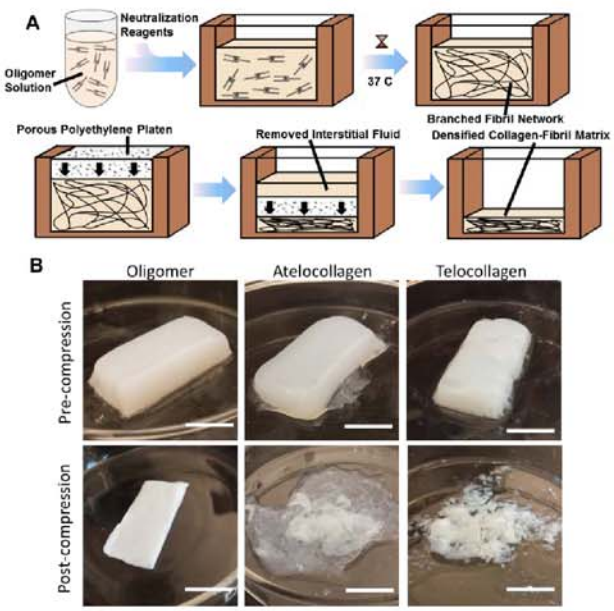

Figure 3 - (A) Process diagram for preparation of densified collagen-fibril constructs. (B) Representative images of oligomer, atelocollagen, and telocollagen constructs (3.5 mg/ml) before and after unconfined 7X compression. Scale bars = 2 mm.

To prepare high-density collagen-fibril constructs, low-concentration collagen matrices were subjected to confined compression using a porous platen, as shown in Figure 3A. Here, the starting concentration of the matrices was held constant but the strain levels varied from (0 to 71 to 86%) to prepare constructs representing final densities of 3.5 mg/ml, 12.25 mg/ml, and 24.5 mg/ml. Interestingly, confined compression of oligomer matrices yielded an intact tissue-like material (Figure 3B). Both confocal and cryo-SEM imaging confirmed that the fibril-microstructure of the densified oligomer constructs remained intact and highly porous (Figure 4). In contrast, the fibril microstructures of telocollagen and atelocollagen could not sustain the compression-induced fluid shear forces and yielded inhomogenous slurries of fluid and fibrillar fragments (Figure 3B). Collectively, these results demonstrate the critical contribution of

suprafibrillar assembly to the overall hierarchical organization and material properties of collagen tissues.

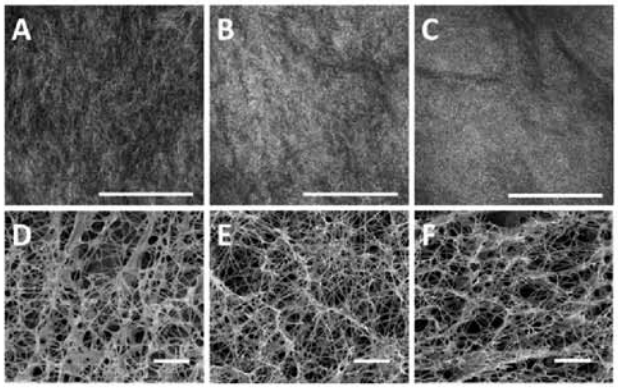

Figure 4 - Fibril microstructure and ultrastructure of collagen constructs prepared at final oligomer concentrations of 3.5 mg/mL (A,D), 12.25 mg/mL (B,E), and 24.5 mg/mL (C,F) as visualized using confocal reflection microscopy (A-C) and cryo-SEM (D-F). Scale bars for A-C and D-F represent 100 μm and 5 μm, respectively.

2.3.2 Controlled Interstitial Fluid Removal Modulates Mechanical Properties and Proteolytic Degradation

The most notable shortcomings of commercial collagen-based materials, whether fashioned from soluble or insoluble collagen formulations, include poor mechanical integrity and rapid proteolytic degradation[3]. As such various approaches, including cell-induced compaction[33] and chemical and physical crosslinking[44] have been routinely applied to improve these properties. Unfortunately, cell-based methods have shown to produce only modest improvements in these performance parameters[33] while exogenous crosslinking methods have been associated with deleterious effects on biocompatibility and inherent biological signaling capacity[45]. Here, we demonstrate how controlled removal of the interstitial fluid phase of oligomer matrices using confined compression

can be used to drastically improve mechanical properties and proteolytic degradability of collagen-fibril materials in absence of exogenous crosslinking and other processing.

Since stress-strain behavior of reconstituted collagen matrices has been shown to be dependent upon polymerization time[17], oligomer matrices were polymerized for 1 hour or 18 hours, prior to densification and follow-up tensile testing. Despite the polymerization time, confined compression resulted in high-density collagen-fibril constructs with increased ultimate strength and elastic modulus. While polymerization time did not significantly affect mean mechanical property values, constructs polymerized for 18 hour showed improved reproducibility as evidenced by reduced standard deviation. As such an 18-hour polymerization time was adopted as a preferred mode.

Comparison of collagen-fibril constructs prepared at 3.5, 12.25, and 24.5 mg/ml showed that both ultimate stress and elastic modulus increased in a nearly linear fashion with collagen content (Figure 5). Ultimate stress values showed statistically significant increases from 65.7 kPa to 120.8 kPa to 212.9 kPa for 3.5, 12.25, and 24.5 mg/mL samples, respectively ($p<0.01$). Likewise, elastic modulus increased in a statistically significant fashion from 0.40MPa to 0.88MPa to 1.26 MPa over the range tested ($p<0.05$; Figure 5). All samples, regardless of densification, failed near 0.28 mm/mm strain (Table 2). The significant contribution of higher-order suprafibrillar assembly to the mechanical properties of densified collagen-fibril constructs is evident upon comparison of results obtained in the present study with oligomer collagen with those obtained with previously with conventional monomer formulations. More specifically, telocollagen required densification via unconfined compression to approximately 100 mg/ml, removing nearly

the entire interstitial fluid component, to yield strength and elastic modulus values seen in this work[11]. Furthermore, conventional collagen materials treated with exogenous chemical crosslinks typically exhibit, on the high end, an elastic modulus of roughly 15-200 kPa, orders of magnitude weaker than the 400 kPa-1.2 MPa observed with oligomeric collagen materials in absence of exogenous crosslinking[46].

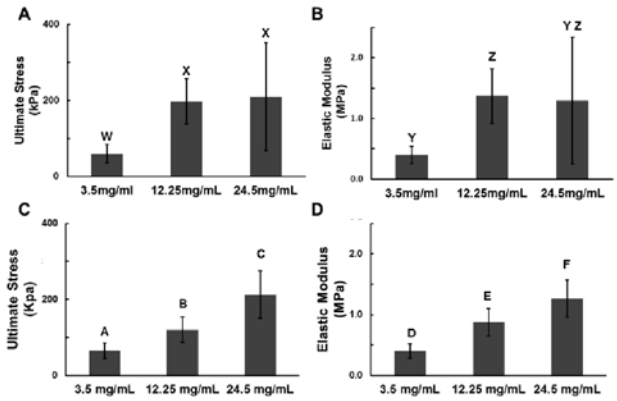

Figure 5 - Engineering tensile mechanical properties of collagen-fibril constructs prepared at oligomer concentration of 3.5 mg/mL, 12.25 mf/mL, and 24.5 mg/mL following 1 hour (A,B) or 18 hour (C,D) polymerization. Dog-bone shaped samples with gauge length, width, and thickness of 10 mm, 4 mm, and 2 mm, respectively, were subjected to uniaxial tensile loading and ultimate stress (A,C), tensile modulus (B,D), and failure strain (not shown) measured (data represents mean±SD; n=7). Letters indicate statistically different groups ($p<0.05$). Table 1 provides summary of all measured values.

Table 2 - Results of Tensile Tests

Collagen Density mg/mL	Engineering Ultimate Stress kPa	Failure Strain mm/mm	Engineering Elastic Modulus Mpa
3.5	65.7±20.4	0.27±0.03	0.40±0.12
12.25	120.8±33.7	0.26±0.04	0.88±0.23
24.5	212.9±62.2	0.30±0.04	1.26±0.31

Densification of collagen-fibril constructs was also found to modulate in-vitro proteolytic degradation properties as measured using collagenase from Clostridium histolyticum. While the specificity of mammalian collagenase is more limited compared to bacterial collagenase, good empirical correlation between the extent of in-vitro degradation by bacterial collagenase and in-vivo degradation by mammalian collagenase has been documented[47]. Qualitative and quantitative assessment of collagenase degradation (Figure 6) showed that the extent of densification affected not only the degradation rate but also to some extent the degradation mechanism (surface versus bulk).

Following 2-hour exposure, the 3.5 mg/mL constructed was nearly entirely degraded, while the 12.25 mg/ml and 24.5 mg/ml constructs showed markedly higher collagenase resistance. Interestingly, 12.25 mg/mL constructs appeared to develop small degraded regions throughout the surface area of the construct, consistent with bulk degradation. In contrast, degradation of the 24.5 mg/mL construct appeared more concentrated to the edges indicative of more limited diffusivity and surface degradation. Proteolytic degradation of the constructs also was defined and compared quantitatively based on the change in compressive modulus before and after 2-hr collagenase treatment (Figure 6B). Here, as shown in Figure 6C, collagenase-treated 3.5 mg/ml constructs showed a dramatic reduction in compressive modulus to 6.7% of untreated controls. In contrast, 12.25 mg/ml and 24.5 mg/ml samples showed significantly reduced levels of collagenase degradation with compressive modulus values of 47% and 71% of untreated controls. The collagenase induced changes in mechanical performance correlated well with collagen content as measured using conventional hydroxyproline assay (Figure 6D).

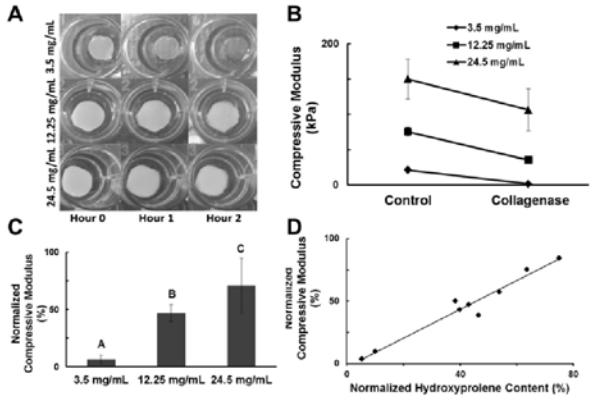

Figure 6 - Density-dependent collagenase degradability of collagen-fibril constructs. (A) Temporal changes in collagen-fibril constructs prepared at 3.5 mg/ml, 12.25 mg/ml, and 24.5 mg/ml following collagenase (31.2 U/ml) treatment. Scale bar = 1 cm. (B) Compressive modulus of untreated (control) and collagenase-treated (2 hr) constructs (data represents mean±SD; n=7). (C) Compressive modulus of collagenase-treated collagen-constructs normalized to control construct values (data represent mean±SD; n=7). Letters indicate statistically different groups ($p<0.05$). (D) Relationship between compressive modulus and hydroxyproline content values for collagenase-treated constructs. Values are normalized to control construct values.

2.3.3 Cellularized High-Density Tissue Constructs and Associated Mechanobiology Signaling

As stated previously, the majority of exogenous crosslinking methods as well as approaches used to achieve high-density collagen constructs compromise cell viability and/or are not amenable to cell encapsulation. Here, we documented the utility of the 2-step confined compression process for creating cellularized, high-density tissue constructs. For these studies, low-density collagen-fibril constructs embedded with hASC were first created and then compressed to various strain levels (Figure 7A). Human ASC were chosen since they represent a relatively abundant multipotent cell type that can be readily harvested from various adipose tissue sites around the body and continues to show promise as a therapeutic cell population for regenerative medicine and

tissue engineering applications[48, 49]. Cell viability, morphology, and F-actin (phalloidin) distribution then were assessed after 48 hours of culture. Control 3.5 mg/mL constructs showed 94.29 ± 2.42% cell viability, while viability within densified 12.25 mg/ml and 24.5 mg/mL constructs was 89.57 ± 2.43 and 88.96 ±2.48%, respectively (Table 3). Although cell viability remained high in all cases, values for densified constructs were statistically lower than the control ($p<0.05$), but not statistically different from each other ($p=0.65$). Collectively, these results document that the compressive loads, fluid shear forces, and high fibril densities do not compromise cell health.

Visualizing F-actin organization (phalloidin) within hASCs encapsulated within various high-density collagen-fibril constructs provided important insights regarding the cell-collagen interactions and associated mechanobiology signaling. The actin cytoskeleton is well recognized for its role in cell morphology as well as establishing physical linkage between the cell interior and collagen fibrils of the extracellular matrix through focal adhesions[50]. Here, encapsulated hASCs were able to sense and respond to the different mechanobiology cues provided by the 3 different collagen constructs as demonstrated by their markedly different morphologies and F-actin distributions (Figure 7C-E). In the control 3.5 mg/mL constructs, cells were spindle-shaped and elongated with prominent actin stress fibers along their long axis. Cells encapsulated within 12.25 mg/ml and 24.5 mg/ml constructs responded to the progressive increase in fibril density and associated matrix stiffness by taking on more stellate and polygonal morphologies, respectively. Furthermore, actin stress fibers became less prominent with the adoption of a more uniformly-distributed, punctate F-actin staining pattern. These morphology and cytoskeletal changes are consistent with previous reports, and reflect modulation of the

cell-matrix tensional balance as occurs with matrices and substrates that are able to resist cell contractile forces[51, 52].

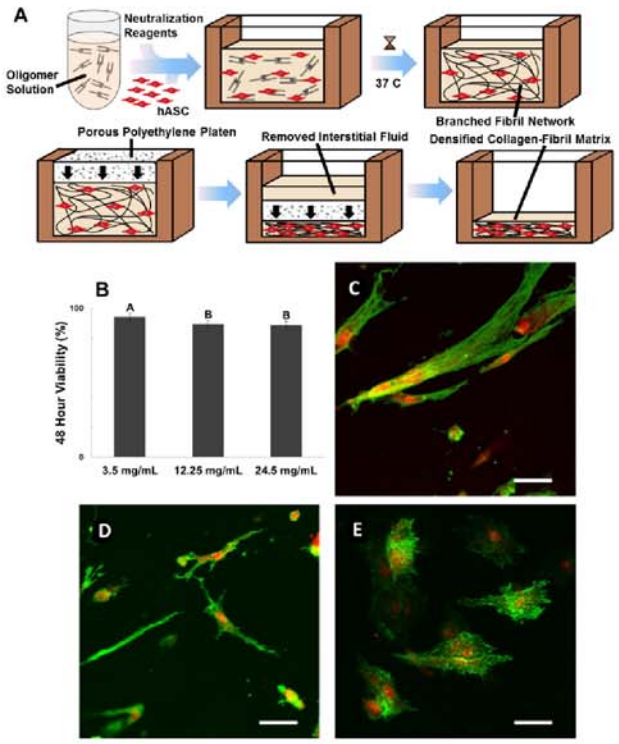

Figure 7 - (A) Process diagram for preparation of cellularized densified collagen-fibril constructs. (B) Cell viability within tissue constructs after 48 hours culture as measured using Celltracker and propidium iodide (data represent mean±SD; n=6). Letters indicate statistically different groups ($p < 0.05$). Representative images hASC within 3.5 mg/mL (C), 12.25 mg/mL (D), and 24.5 mg/mL (E) constructs stained with phalloidin (green) and DRAQ5 (red), and visualized using confocal microscopy. Images represent 2D projections of image stacks (50 µm). Scale bars = 50 µm

Table 3 - 48 Hour Viability Testing

Collagen Concentration mg/mL	Viability % Live
3.5	94.29 ± 2.42 A
12.25	89.57 ± 2.43 B
24.5	88.96 ± 2.48 B

2.4 Conclusion

The development of functional tissue constructs for research and medical applications requires an in-depth understanding of how cells interact and respond to the surrounding extracellular matrix. Since collagen exists in vivo as fibers and is the major component of connective tissue, oligomeric collagen-fibril matrices provide a highly physiologically relevant system. A key finding of this work is the benefit of oligomers and their associated suprafibrillar assembly capacity for creating acellular or cellular collagen-fibril constructs with tissue-like appearance, handling, and performance. Densification of oligomer collagen matrices irreversibly removed a portion (71-86%) of the fluid from the material, reproducibly creating novel materials with the collagen concentration and strength of soft connective tissues. The material is capable of being made without the use of any exogenous crosslinking chemicals or matrix destroying processes, retaining the collagen's in vivo branched fibril microstructure. The densification process was shown to be amenable to creating high density cellularized tissue constructs. This material, with its hierarchical tuning capability of material properties, shows large promise for tissue engineering applications and basic science studies, such as three dimensional cell culture.

CHAPTER 3. TRANSLATIONAL DESIGN ASPECTS OF HIGH-DENSITY COLLAGEN-FIBRIL CONSTRUCTS

3.1 Introduction

Collagen is the major structural element of connective tissues and the prominent component of the extracellular matrix. Its suprafibrillar assembly and hierarchical organization varies from tissue to tissue bringing diversity in form and function[1]. In addition to conferring structure and mechanical properties to the body's tissues and organs, this natural polymer has been more recently recognized for its critical role in cellular signaling associated with tissue development, maintenance, and repair[53]. Both in-vitro and in-vivo studies have shown that the collagen fibril microstructure and stiffness of the cell microenvironment provide important guidance cues that regulate not only fundamental behavior of differentiated cells but also differentiation and morphogenesis of multipotent stem cells[54]. Instrumental to this mechanobiology signaling are molecular signaling domain for cell adhesion, proteolytic degradation, and growth factor binding inherent to the tropocollagen molecule, which represents the fundamental collagen building block[55].

The clinical applications of collagen have been limited by the non-*in vivo* like state of collagen products. To date, collagen-based material and tissue design for both research and medical applications has relied on a limited number of collagen

formulations known to vary in purity and biomechanical and biochemical signaling capabilities. A variety of collagen materials have seen extensive clinical use as biodegradable hemostatic agents, bulking agents for plastic surgery, wound coverings and, more recently, as biodegradable drug delivery vehicles[3]. Formulations used to date include purified collagen gels, decellularized matrices, and fibrillary collagen sponges. These materials create a more biological interface between the body and the wound, aiding the healing process. Due to the biodegradability of the collagen, which is lessened by crosslinking through physical or chemical means in some forms, the materials can be left in after surgery and slowly degraded and removed from the body with minimal adverse reactions[15]. However, the clinical uses of collagen to date do not readily take advantage of the biomechanical and biochemical signaling capabilities of the collagen.

Collagen has seen extensive use, particularly in research applications, in the form of purified collagen solutions which can form gels. This form of collagen has the clinical advantage of being injectable, and forming a gel within the body. However, the dissolved collagen solutions are limited in concentration by solubility, and are traditionally monomeric collagen formulations[5]. Monomeric collagen formulations lack the natural intermolecular crosslinks found in in vivo collagen, severely limiting the polymerization capacity of the solution as well as the mechanical integrity of the polymerized gel[18]. Films of collagen have been used in combination with other materials or cells as a treatment for burns, due to their impermeability to bacteria and low antigenicity[14, 56].Soluble, polymerizable monomeric collagen has been used in combination with cells in an FDA approved skin substitute under the trade name of Apligraf. Apligraf consists of a collagen matrix which has been contracted by human fibroblasts. This method of action,

cellular contraction, to create a higher collagen fibril density matrix functions due to the inherent weakness found in these monomeric collagens, which allows the force of the cells to tightly contract the matrix. In addition, the inclusion allogenic cells can illicit an immunogenic response from the recipient.

In order to overcome the low mechanical integrity of collagen formulations, decellularized tissues have been used. These materials consist of the extracellular matrices of natural tissues, such as small intestine or urinary bladder, with the cells removed, retaining the mixture of proteins naturally found in the donor site[13]. Other tissue sources used include heart valves, skin, and skeletal muscle[3]. However, these materials are subject to more inherent variability, as the individual differences between donor sites are not removed. As such, the microstructure, protein makeup, and mechanical properties are all subject to variances in the humans and animals they are obtained from[57]. These products can also be exogenously crosslinked to gain higher mechanical integrity, but at the cost of the natural biochemical signaling capabilities of that tissue.

Insoluble collagens (also referred to as fibrillar collagens) that don't polymerize are routinely fashioned into high-density, porous collagen sponges through lyophilization of collagen slurries. To create these products, tissue sources high in collagen content, such as tendon, are milled into particulate, washed to remove excess proteins such elastin, crosslinked, frozen, and lyophilized. Overall, these materials have amorphous (non-fibrillar) microstructures and are often further subjected to exogenous chemical or physical crosslinking to improve mechanical properties and decrease proteolytic

degradability. The collagen causes platelets to clot upon contact, allowing control over blood loss during surgery[58].

The collagen sponges have also seen recent clinical use as drug delivery vehicles for a number of drugs, including gentamicin and rh-BMP2[15]. In these forms, the lyophilized collagen sponge is soaked in solution containing the drug prior to implantation in the body. The sponge is then degraded by the body, allowing some extended release of drug into the body, and the collagen sponge is degraded and removed from the body over time.

In short, the currently available collagen formulations lack the in vivo microstructure, resistance to degradation, and mechanical integrity of natural collagen, and in order to regain some of the lost mechanical integrity, as in exogenous crosslinking, the natural microstructure is further damaged. This process leaves the collagen materials with properties that are far exceeded by the natural collagen, and are unfit to guide cellular fate and behavior in a clinically relevant fashion. This lack of a physiologically relevant form of processed collagen must be overcome to take clinical advantage of the collagen's biochemical and biophysical signaling capabilities for tissue engineering and regenerative medicine applications.

Recently, we described the isolation and purification of type I collagen oligomers, which appear to represent a new soluble subdomain that falls between molecular and fibrillar size scales[6]. Oligomers represent aggregates of tropocollagen molecules (e.g., trimer) that retain their natural intermolecular crosslink. More specifically, characterization studies performed to date suggest that oligomers purified from porcine dermis represent a prong-shaped molecule in which three molecules are covalently

connected at α1-Hyl 87, α2-His 92, and α1-Lysald 16c amino acid residues by the histidinohydroxylysinonorleucine crosslink[18, 59]. Unlike conventional collagen monomers, oligomers exhibit rapid fibril and suprafibrillar self-assembly yielding highly interconnected collagen-fibril matrices with dramatically improved mechanical integrity, handling, and reduced proteolytic degradation. More recently, low-density matrices were found to exhibit plastic deformation when subjected to confined compression, creating high density (>10 mg/mL) collagen-fibril materials that appear and handle like soft connective tissues and support cell encapsulation. More specifically, the plastic deformation created collagen fibril materials with tunable elastic moduli ranging from 400 kPa to 1.3 MPa, with 90% cell viability exhibiting different encapsulated hASC morphology at 48 hours post-densification. The process was also found to be capable of creating gradients in collagen fibril density and alignment.

Here we extend this work by evaluation lyophilization as a means to promote stability, preserve biological function, and facilitate long-term storage of high-density collagen-fibril materials. Lyophilization represents the current industry standard for prolonging the shelf life of collagen and other biologically based materials[60]. Studies involved high density collagen-fibril materials, representing 24.5 mg/mL oligomeric collagen. Multi-scale structural properties, mechanical behavior, and proteolytic degradation are compared before and after lyophilization and rehydration. In addition, this high density collagen-fibril material is compared to Helistat, a commercial collagen sponge used for hemostasis and drug delivery[15, 61]. Results document how the suprafibrillar assembly of collagen oligomers dramatically improves the mechanical

integrity of biosynthetic collagen biomaterials while maintaining a highly porous collagen-fibril microenvironment with tunable mechanobiology signaling.

3.2 Materials and Methods

3.2.1 Preparation of High-Density Oligomer Collagen-Fibril Materials

Type I collagen oligomers were acid solubilized from dermis of market weight pigs and lyophilized for storage as described previously[6]. Prior to use, lyophilized collagen was dissolved in 0.01 N hydrochloric acid (HCl) and rendered aseptic by chloroform exposure at 4°C. Collagen concentration was determined using a Sirius Red (Direct Red 80) assay [30]. The oligomer formulation was standardized based upon purity as well as polymerization capacity according to ASTM standard F3089-14 [38]. Here, polymerization capacity is defined by matrix shear storage modulus (G') as a function of collagen concentration of the polymerization reaction. Oligomer solutions were diluted with 0.01 N HCl to achieve desired concentrations and neutralized with 10X phosphate buffered saline (PBS) and 0.1N sodium hydroxide (NaOH) to achieve pH 7.4 [18]. Neutralized solutions were kept on ice prior to inducing polymerization by warming to 37^{o}C.

Oligomer collagen-fibril matrices were prepared with an initial starting collagen concentration of 3.5 mg/ml in 2 cm X 4 cm block molds. After polymerization and incubation at 37°C for 18 hours, each matrix was compressed within the block mold to a final thickness of 2 mm (1.6 mL volume) with a porous polyethylene platen (50 µm pore size; Scientific Commodities, Inc., Lake Havasu City, AZ) at a rate of 6 mm/min. Final

collagen concentration was controlled by varying the initial polymerized collagen volume. More specifically, a starting volume of 11.2 mL of 3.5 mg/mL collagen (initial concentration) were compressed to yield 24.5 mg/mL (86% strain) constructs. Commercial Collagen sponges (Helistat) were purchased from Miltex (York, PA).

3.2.2 Collagen Biomaterial Micro- and Ultrastructure Analysis

The fibril micro- and ultra-structure of the commercial Helistat collagen sponge and oligomer collagen-fibril materials were visualized using SEM as well as cryo-SEM. SEM and Cryo-SEM images of samples were obtained using an FEI NOVA nanoSEM 200 (FEI, Hillsboro, OR). Lyophilized samples were mounted and sputter coated under vacuum prior to imaging. Rehydrated samples were quick frozen by submersion into liquid nitrogen cooled to its triple point, transferred to a CT1000 coldstage attachment (Oxford Instruments North America, Inc., Concord, MA), and sublimated under vacuum before sputter coating and imaging.

3.2.3 Mechanical Testing

Tensile testing was performed on dog-bone shaped rehydrated collagen constructs with a gauge length, width, and thickness of 26 mm, 4 mm, and 2 mm, respectively. All samples were tested in uniaxial tension to failure at a strain rate of 10 mm/second using a servo electric materials testing system (Testresources, Shakopee, MN). Stress measurements were obtained using a 10 lb load cell (LPM 512, Cooper Instruments, Warrenton, VA) at a sampling rate of 100 Hz. Engineering tensile modulus (E_T) was calculated from the linear region of the stress strain curve. Ultimate stress (σ_U)

represented peak stress experienced by the sample, and failure strain (ε_f) was the strain at which constructs experienced total failure. (n=7).

3.2.4 Suture Retention

Helistat collagen sponges and lyophilized high-density oligomer collagen-fibril matrices were hydrated and their suture retention strength quantified according to ASTM standard protocol STP898[62]. Prolene suture (5-0) was looped through the material at a "bite distance" (distance between the edge of the material and the suture) of 1.5 mm [7]. The suture then was looped through a hook connected to a servo electric materials testing system (Testresources, Shakopee, MN) and tied using several square knots to prevent slipping. The suture was then pulled by the tensile tester at a crosshead speed of 25.4 mm/min until failure, and the peak force was recorded in grams. Force measurements were obtained using a 10 lb load cell (LPM 512, Cooper Instruments, Warrenton, VA) at a sampling rate of 100 Hz. (n=7).

3.2.5 Proteolytic Degradability

Proteolytic degradation was assessed by measuring compressive modulus of constructs before and after 2-hour exposure to bacterial collagenase type IV (31.2 U/mL; Worthington, Lakewood, NJ). Helistat collagen sponge and oligomer collagen-fibril material (24.5 mg/ml) were punched to form cylinders with diameter and thickness of 1 cm and 2 mm, respectively. Constructs were tested in unconfined compression at 17%/second to 75% strain using a servo electric materials testing system (Testresources, Shakopee, MN) adapted with a 10 lb load cell (LPM 512, Cooper Instruments, Warrenton, VA). Compressive modulus was calculated as the slope of the linear region of the stress-

strain curve. Compression tests were performed on seven independent constructs per group (n=7).

3.2.6 Statistical Analysis

For each measure, two-sided t-tests were performed between the high-density oligomer collagen-fibril matrices and the commercial collagen sponges with a critical p-value of 0.05.

3.3 Results and Discussion

3.3.1 Rehydrated High-Density Oligomer Collagen-Fibril Matrices

3.3.1.1 Ethanol Rehydration Preserves Marcrostructure and Ultrastructure

Lyophilization is a useful tool for prolonging the shelf life of collagen or other biologically based materials. Lyophiliztion of decellularized urinary bladder extracellular matrix was found to have minimal effects on the mechanical properties over a year after the lyophilization occurred, whether stored in a room temperature or refrigerated environment[63]. When rehydrated using water or 1X phosphate buffered saline, the high-density oligomer collagen-fibril matrices experienced macrostructure collapse, decreasing in thickness from 2 mm to approximately 0.4 mm. When first subjected to the short incubation in ethanol, the high-density oligomer collagen-fibril matrices retained their macrostucture thickness of 2 mm. This pattern was examined using graded mixtures of ethanol in water, and showed that at $\leq$10% ethanol by volume, a surface tension of 48 mN/m[64], the solution caused collapse of the high-density oligomer collagen-fibril matrix, while at $\geq$20% ethanol by volume, a surface tension of 39 mN/m[64] the structure did not

collapse (Figure 8). During rehydration with water only, the rehydration and collapse took place over a long period of time, on the order of an hour. Ethanol rehydration, in contrast, was complete in under one minute, and the replacement of ethanol with water when placed in the water bath happened over a short timescale as well, complete in under 5 minutes.

The differences in rehydration are likely due to the effect of the surface tension on the fibril microstructure of the oligomeric collagen, as limiting osmotic forces and surface tension are critical for optimal rehydration. Ethanol in particular has previously been shown to be a useful tool in the rehydration of chitosan scaffolds[65]. Under rehydration with solutions with relatively high surface tension, the fibrils are bent and buckled by the incoming force of the fluid, collapsing the structure. When rehydrated using solutions with low surface tension, such as ethanol, the force on each fibril is low enough for the microstructure to withstand the force of the incoming fluid.

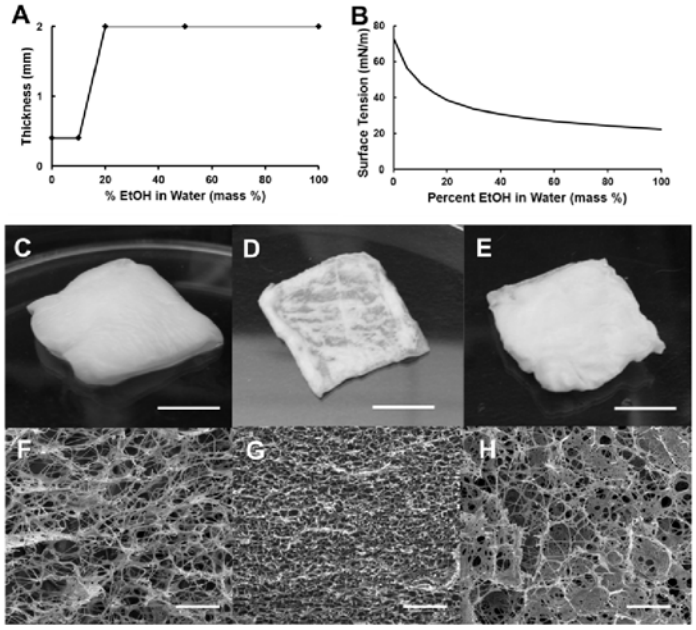

Figure 8 - Collagen-fibril materials that were lyophilized and then rehydrated displayed material properties that were dependent upon the surface tension of the rehydration solution. Plots of material thickness following rehydration as a function of ethanol-water percentage (A) and associated solution surface tension as a function of ethanol-water percentage (data adapted from [17]) (B). Representative collagen-fibril materials and associated CryoSEM ultrastructure before lyophilization (C,F); after lyophilization and rehydration in water (D,G); and after lyophilization and rehydration in ethanol (E, H). Materials rehydrated in ethanol maintained their shape and microstructure while those rehydrated in water collapsed. Scale bars are 1 cm (C - E) and 5 um (F - H).

The high-density oligomer collagen-fibril matrix, when lyophilized, showed an open ultrastructure composed of an interconnected fibril network. When rehydrated using only water or PBS, the ultrastructure was affected, creating a much denser network of fibrils, although smaller continuous pores through the material were still observed. When rehydrated with an initial incubation in ethanol, the ultrastructure of the high-density

oligomer collagen-fibril matrix was very similar to that seen in the lyophilized oligomer sponge, being made up of an interconnected, branched collagen fibril network.

3.3.1.2 Mechanical Properties of Rehydrated High-Density Oligomer Collagen-Fibril Matrices

The high-density oligomer collagen-fibril matrices showed an average ultimate tensile stress of 196.9 ± 66.0 kPa, failure strain of 0.33 ± 0.03 mm/mm, and elastic modulus of 1.29 ± 0.52 MPa. The ultimate stress, failure strain, and elastic modulus of the rehydrated high-density oligomer collagen-fibril matrix were all found to be statistically similar to those of the oligomeric collagen of identical preparation that had not undergone a lyophilization procedure. The suture retention strength of the high-density oligomer collagen-fibril matrix was 0.54 ± 0.16 N. Data summarized in Figure 9. The oligomeric collagen was found to have a statistically similar suture retention strength to the rehydrated high-density oligomer collagen-fibril matrix, with a suture retention strength of 0.65 ± 0.21 N. Overall, no differences were found between the mechanical properties of the hydrated and rehydrated high-density oligomer collagen-fibril matrices. The properties of the polymerized high-density oligomer collagen-fibril matrix are orders of magnitude higher than the 1-30 kPa elastic modulus seen in polymerized monomeric collagen formulations[6]. In addition, the elastic modulus values are similar to those seen for SIS (0.8-1.6 MPa), a commonly used decellularized tissue product[66].

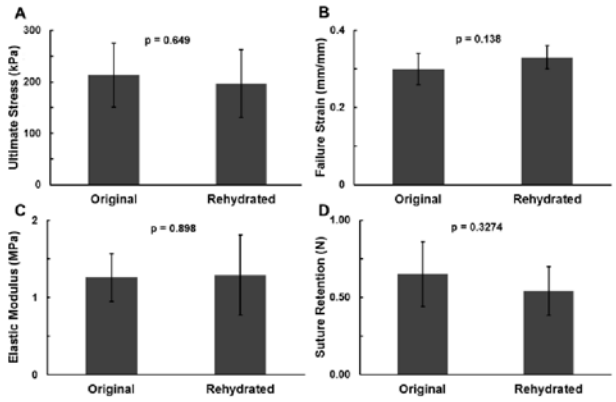

Figure 9 - Engineering tensile mechanical properties of high-density collagen-fibril materials before (original) and after lyophilization and rehydration (rehydrated). Dog-bone shaped samples with gauge length, width, and thickness of 10 mm, 4 mm, and 2 mm, respectively, were subjected to uniaxial tensile loading and ultimate stress (A), failure strain (B), and tensile modulus (C) measured. Retention strength (D) measured using 5-0 prolene suture with a 1.5 mm bite distance. Data represents mean±SD; n=7.

3.3.1.3 Proteolytic Degradation Properties of High-Density Oligomer Collagen-Fibril Matrices

The compressive moduli before and after proteolytic degradation for the high-density oligomer collagen-fibril matrix were 157.5 ± 47.2 kPa and 109.2 ± 27.8 kPa, respectively, resulting in 69.3 ± 27.3 % of the compressive modulus remaining after degradation (Figure 10). The compressive moduli before and after degradation and the percentage remaining for the high-density oligomer collagen-fibril matrix were all found to be statistically similar to the values for the oligomeric collagen that had not undergone the lyophilization process. This result suggests that the lyophilization and rehydration procedures, including the ethanol incubation, did not significantly affect the chemical structure of the collagen fibrils, as they still showed the same proteolytic degradation

profile. The compressive moduli is also orders of magnitude higher than the <5 kPa compressive moduli seen for polymerized monomeric collagens[6].

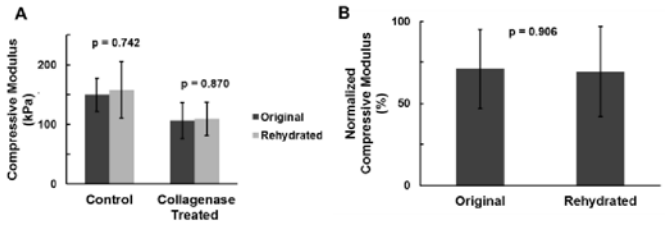

Figure 10 - A) Compressive modulus of untreated (control) and collagenase-treated (2 hr) samples of high-density collagen-fibril materials before (Original) and after lyophilization and rehydration (Rehydrated). B) Post-degradation compressive moduli normalized by the control compressive moduli. Data represents mean±SD; n=7.

3.3.2 Comparison Commercial Collagen Sponges

3.3.2.1 Macrostructure and Ultrastructure

The Helistat commercial collagen sponges showed no preference for rehydration treatment, quickly absorbing the fluid without change to its macrostructure dimensions. The differences seen between the rehydration properties of the oligomeric and commercial collagen sponges are likely due to differences in their microstructures (Figure 11). The high-density oligomer collagen-fibril matrix is made up of an interconnected branched fibril network. This highly porous network results in each fibril having some distance from its neighbors. The Helistat collagen sponge, in contrast, is made up of tightly packed bunches of crosslinked fibrils separated by wide open pores of several hundred microns. This results in the solid portions of the matrix having much higher bulk strength than the individual fibrils, allowing them to resist the forces of fluid rehydration.

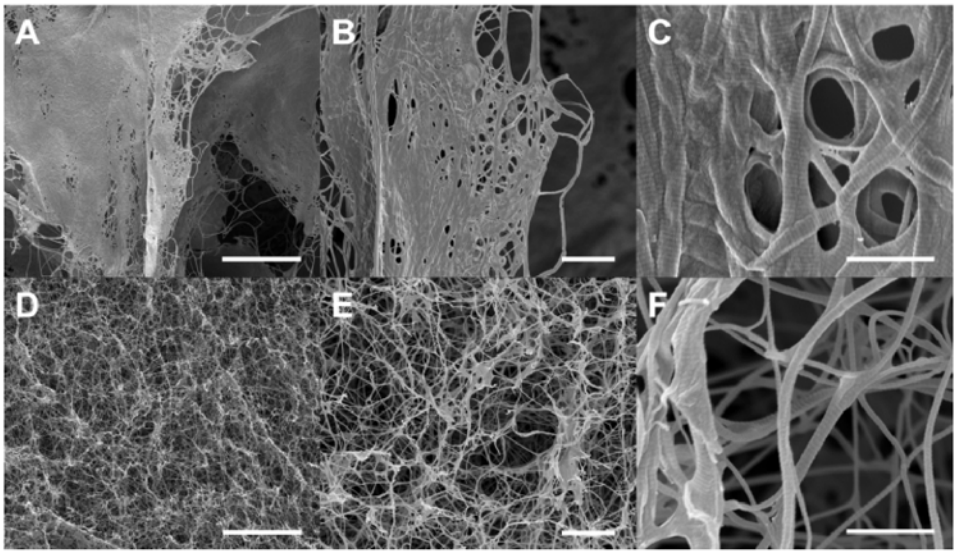

Figure 11 - Ultrastructure of Helistat (A-C) and lyophilized high-density collagen-fibril material as visualized using SEM (D-F). Helistat represents disconnected regions of tissue-derived ECM while high-density collagen-fibril material represents a highly interconnected self-assembled fibril network derived from soluble oligomeric collagen. Note that component fibrils in both materials show characteristic collagen D-banding (C & F). Scale bars are 30 um, 5 um, and 1 um, respectively.

Both the high-density oligomer collagen-fibril matrix and the Helistat demonstrated the characteristic d-banding of collagen under SEM imaging (Figure 11C and 11F). This is expected from the Helistat as it is created from a microfibrillar grinding process and crosslinking and lyophilization of the resulting slurry, without destroying or dissolving the original collagen fibrils. In the high-density oligomer collagen-fibril matrices , which are created through the dissolution collagen followed by polymerization at a later time point, the d-banding shows evidence that the oligomeric collagen is capable of self-organizing into collagen's *in vivo* state, which is not seen in the polymerization of atelocollagen[53]. In addition, the ultrastructure of the high-density oligomer collagen-fibril matrix matches that seen in connective tissues in the body, being comprised of an interconnected, dense, branched fibril network. The Helistat's

ultrastructure was shown to be made up of regions of dense compacted fibrils separated by large pores up to several hundred microns across.

3.3.2.2 Mechanical Properties

The Helistat commercial collagen sponges showed an average ultimate tensile stress of 47.8 ± 7.4 kPa, failure strain of 0.32 ± 0.08 mm/mm, and elastic modulus of 0.27 ± 0.03 MPa. Data shown in Figure 12. The high-density oligomer collagen-fibril matrix was found to have statistically significantly higher values for ultimate stress and elastic modulus, and a statistically similar value for failure strain. The high-density oligomer collagen-fibril matrix having an order of magnitude higher elastic modulus than the Helistat is quite noticeable considering the high-density oligomer collagen-fibril matrix contains no exogenous crosslinking, while the Helistat is formaldehyde crosslinked. This increased elastic modulus also brings the material properties of the high-density oligomer collagen-fibril matrix into the realm of soft tissues found in the body, implying its usefulness in reconstructive surgery as a tissue replacement. The suture retention strength of the Helistat commercial collagen sponge was 0.34 ± 0.08 N. The high-density oligomer collagen-fibril matrix was found to have a statistically significantly higher suture retention strength, although both fall short of the generally accepted 2N requirement for surgical use[67]. The elastic modulus of the Helistat is similar to the 50-200 kPa elastic modulus reported for collagen-GAG sponges crosslinked with dehydrothermal treatment, UV irradiation, and/or glutaraldehyde[68]. Overall, the high-density oligomer collagen-fibril matrix was shown to have nearly double the suture

retention capability of the commercially available collagen sponge, aiding itself to better use as a soft connective tissue replacement.

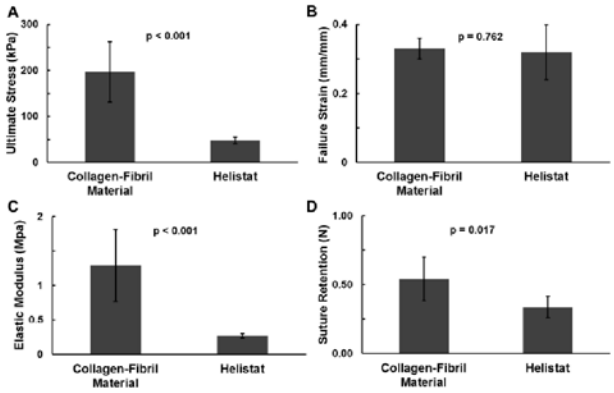

Figure 12 - Engineering tensile mechanical properties of rehydrated high-density collagen-fibril material and Helistat collagen sponge. Dog-bone shaped samples with gauge length, width, and thickness of 10 mm, 4 mm, and 2 mm, respectively, were subjected to uniaxial tensile loading and ultimate stress (A), failure strain (B), and tensile modulus (C) measured. Retention strength (D) measured using 5-0 prolene suture with a 1.5 mm bite distance. Data represents mean±SD; n=7.

3.3.2.3 Proteolytic Degradation

The compressive moduli before and after proteolytic degradation for the Helistat commercial collagen sponge were 16.9 ± 3.2 kPa and 13.8 ± 1.8 kPa, respectively, resulting in 81.9 ± 18.5 % of the compressive modulus remaining after degradation. The compressive moduli values for the high-density oligomer collagen-fibril matrix were an order of magnitude larger both before and after proteolytic degradation (Figure 13). While the percentage of the original compressive modulus remaining was higher on average for the Helistat commercial collagen sponge, the two values were not statistically significantly different. The compressive modulus of the high-density oligomer collagen-fibril matrix was found to be an order of magnitude higher than that of the Helistat. The

drastic increase in compressive modulus and similarity in resistance to proteolytic degradation are substantial in regards to the insight that the high-density oligomer collagen-fibril matrix contains no exogenous crosslinking, instead relying solely on the *in vivo* like branched collagen fibril network for mechanical integrity.

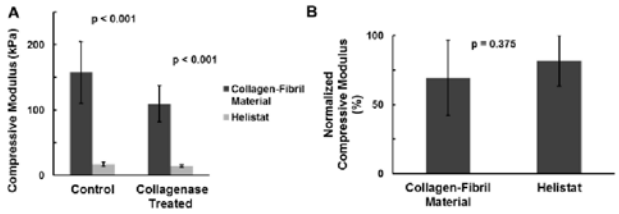

Figure 13 - A) Compressive modulus of high-density collagen-fibril materials and helistat before (control) and after 2-hr collagenase treatment (Collagenase-Treated). B) Normalized compressive modulus for collagenase treated collagen-fibril materials and helistat. Data represents mean±SD; n=7.

The comparative resistance is of particular importance when it is noted that the high-density oligomer collagen-fibril matrix has undergone no exogenous crosslinking, while the Helistat has undergone formaldehyde crosslinking, which is known to decrease the biological degradability of fibrillary collagen sponges to around 1% of its original value[69]. Having a similar amount of degradation resistance without the formaldehyde treatment lends further credence to the mechanical integrity and fibril stability granted by the use of collagen oligomers over traditional fibrillary or monomeric collagens.

3.4 Conclusions

The high-density oligomer collagen-fibril matrix is made up of an interconnected branched collagen fibril network, with collagen content and ultrastructure resembling that found in soft tissues. The elastic and compressive material properties were found to be an order of magnitude higher than those found in the commercial collagen sponge, reaching

those levels found in soft tissues. This is important as the mechanical properties of the extracellular matrix have been found to have an overwhelming effect on the cells that interact with it, so much so that the mechanical cues can override the signals given by soluble factors *in vitro*. Even more notable is that the high-density oligomer collagen-fibril matrix was capable of achieving such high mechanical properties without the need for exogenous aldehyde crosslinking, which is known to have deleterious effects on the biological signaling capabilities of collagen, as well as potentially harmful cellular responses[45]. The creation of a tissue-like collagen sponge material which can be lyophilized and stored for long periods before use as a tissue replacement could have great utility as a soft tissue replacement for mastectomies, or as a tissue replacement for deep burn wounds or ulcers. These materials may allow for full integration into the patient and allow for exemplary healing. In the cases of hard tissue replacement and void filling, such as bone, the increased material properties will likely lead to more adequate bone formation due to the strength and density of the matrix giving cues to the natural osteoclasts and osteoblasts responsible for bone growth and repair. These claims require further study into the *in vivo* behavior of these high-density oligomer collagen-fibril matrices.

The use of ethanol as a rehydrating agent allowed the collagen materials to retain their pre-lyophilization ultrastructure and mechanical properties. Ethanol is often used in the laboratory setting as a sterilization solution, and has been shown to have limited effects on the properties of collagen matrices[68].

Overall, the materials created for this study provide the controllable microstructure and repeatability of polymerizable collagen, the natural biophysical

signaling properties and mechanical properties of decellularized tissue, and the long term storage and ease of use of fibrillary collagen sponges, without the need for any exogenous crosslinking.

It should be noted that the high-density oligomer collagen-fibril matrix has not undergone sterilization, as the Helistat has, and this has been known to have an effect on the mechanical properties of collagen based products. However, the effects of sterilization, and in particular ETO sterilization which is commonly used for collagen based products, have been non-substantial changes in integrity, cellular proliferation, or proteolytic degradation, and an increase in tensile strength.

CHAPTER 4. CONCLUSION

4.1 Conclusions

The oligomeric collagen formulations have a distinct advantage over other monomeric collagen formulations because of their innate ability to self-assemble into branched fibril networks similar to those found in collagen in vivo. This microstructure shows drastic mechanical integrity improvements over monomeric collagens. The high mechanical integrity allows the oligomeric collagen gels to withstand a forced removal of a portion of the interstitial fluid phase, plastically creating materials with a much higher collagen fibril density and increased material properties.

The densification technique created materials with controlled high level biophysical properties, including order of magnitude increases in elastic and compressive moduli, as well as increases in resistance to proteolytic degradation. The process was found to be amenable to cell encapsulation, creating high density cellularized tissue constructs which could impart controlled biomechanical cues to the encapsulated cells.

The densified collagen oligomer materials were capable of withstanding a lyophilization procedure, and could be rehydrated without an effect on the mechanical or biochemical properties of the collagen by utilizing an ethanol rehydrating solution.
The high-density collagen-fibril materials were found to have significantly higher elastic and compressive mechanical properties than a commercial, crosslinked, fibrillar collagen

sponge. The proteolytic degradation properties of the two materials were statistically similar, quite interesting considering the high-density collagen-fibril material contains no crosslinking to limit the biological activity of the collagen. Overall the high-density collagen-fibril material shows excellent promise as a clinical tool for tissue engineering applications.

Overall, the materials created for this study provide the controllable microstructure and repeatability of polymerizable collagen, the natural biophysical signaling properties and mechanical properties of decellularized tissue, and the long term storage and ease of use of fibrillary collagen sponges, without the need for any exogenous crosslinking.

4.2 Future Directions

The mechanical integrity differences between the monomeric and oligomeric collagen formulations provide an outlook for further studies. In particular, a combination of monomeric collagens and oligomeric collagens combined with the densification technology explored here could create materials with high level collagen fibril densities with a range of material properties. This research could add a further level of individual property control for tissue engineering applications.

The increased collagen density provided by the densification allows for the creation of cellularized in vitro tissue constructs for basic science studies. Because the cell-matrix interactions have a drastic effect on cell proliferation and differentiation, creation of an in vivo-like microstructure is paramount to an in vitro understanding of how cells behave in vivo. This technique, densification of oligomer collagen matrices, could allow for studies

of the effects of high collagen density microstructures on stem cell fate, or allow for the creation of more bone-like microstructures for study. In addition, this technology could allow for the creation of cryopreserved high density tissue constructs.

In order to further examine the clinical potential of the high-density collagen-fibril materials, in vivo studies are necessary. Evaluating how the sponges fair in an in vivo environment with further elucidate the effects the branched fibril network and high collagen fibril density can have on wound healing.

In addition, the effect of sterilization on the high-density collagen-fibril materials is necessary to evaluate how the biophysical properties change through this process. ETO sterilization is the current industry gold standard for collagen based products, and has been shown to have limited effects on the properties of the materials. So, it is likely that ETO sterilization will be adequate for use on the high-density collagen-fibril materials and will not cause destruction of the biophysical properties.

BIBLIOGRAPHY

BIBLIOGRAPHY

1. D. J. S. Hulmes, *Journal of Structural Biology*, 2002, **137**, 2–10.
2. F. W. K. Lisa D. Muiznieks, *Biochimica et Biophysica Acta (BBA) - Molecular Basis of Disease*, 2013, **1832**, 866–875.
3. E. A. Abou Neel, L. Bozec, J. C. Knowles, O. Syed, V. Mudera, R. Day and J. K. Hyun, *Adv Drug Deliv Rev*, 2013, **65**, 429-456.
4. *Collagen - Structure and Mechanics | Springer*, 2015.
5. C. F. Whittington, E. Brandner, K. Y. Teo, B. Han, E. Nauman and S. L. Voytik-Harbin, *Microsc Microanal*, 2013, **19**, 1323-1333.
6. S. Kreger, B. Bell, J. Bailey, E. Stites, J. Kuske, B. Waisner and S. Voytik-Harbin, *Biopolymers*, 2010, **93**, 690-707.
7. A. M. Pizzo, K. Kokini, L. C. Vaughn, B. Z. Waisner and S. L. Voytik-Harbin, *Journal of Applied Physiology*, 2005, **98**, 1909-1921.
8. M. M. G. Guille, C. Helary, S. Vigier and N. Nassif, 2010, **6**, 4963-4967.
9. C. S. Hughes, L. M. Postovit and G. A. Lajoie, *PROTEOMICS*, 2015, **10**, 1886-1890.
10. M. M. Giraud-Guille, *International review of cytology*, 1996, **166**, 59-101.
11. R. Brown, M. Wiseman, C. Chuo, U. Cheema and S. Nazhat, *ADV FUNCT MATER , 15 (11) 1762 - 1770. (2005)*, 2005, **15**, 986-992.
12. M. Bitar, V. Salih, R. A. Brown and S. N. Nazhat, *J Mater Sci Mater Med*, 2007, **18**, 237-244.
13. F. Moroni and T. Mirabella, *Am J Stem Cells*, 2014, **3**, 1-20.
14. *Burns*, 2003, **29**, 837–841.
15. M. Geiger, R. H. Li and W. Friess, *Adv Drug Deliv Rev*, 2003, **55**, 1613-1629.
16. L. Bessea, B. Coulomb, C. Lebreton-Decoster and M. M. Giraud-Guille, *Biomaterials*, 2002, **23**, 27-36.
17. B. A. Roeder, K. Kokini, J. E. Sturgis, J. P. Robinson and S. L. Voytik-Harbin, *J Biomech Eng*, 2002, **124**, 214-222.
18. J. L. Bailey, P. J. Critser, C. Whittington, J. L. Kuske, M. C. Yoder and S. L. Voytik-Harbin, *Biopolymers*, 2011, **95**, 77-93.
19. J. Lee, A. A. Abdeen, D. Zhang and K. A. Kilian, *Biomaterials*, 2013, **34**, 8140-8148.
20. S. Khetan, M. Guvendiren, W. R. Legant, D. M. Cohen, C. S. Chen and J. A. Burdick, *Nat Mater*, 2013, **12**, 458-465.
21. T. Mammoto, A. Mammoto and D. E. Ingber, *http://dx.doi.org/10.1146/annurev-cellbio-101512-122340*, 2013.

22. S. M. Sweeney, J. P. Orgel, A. Fertala, J. D. McAuliffe, K. R. Turner, G. A. D. Lullo, S. Chen, O. Antipova, S. Perumal, L. Ala-Kokko, A. Forlino, W. A. Cabral, A. M. Barnes, J. C. Marini and J. D. S. Antonio, *Journal of Biological Chemistry*, 2008.
23. D. J. Hulmes, A. Miller, D. A. Parry, K. A. Piez and J. Woodhead-Galloway, *J Mol Biol*, 1973, **79**, 137-148.
24. E. K. H. David L. Christiansen, Frederick H. Silver, *Matrix Biology*, 2000, **19**, 409–420.
25. A. J. Bailey, R. G. Paul and L. Knott, *Mech Ageing Dev*, 1998, **106**, 1-56.
26. D. R. Eyre, M. A. Paz and P. M. Gallop, *Annu Rev Biochem*, 1984, **53**, 717-748.
27. L. C. Abraham, E. Zuena, B. Perez-Ramirez and D. L. Kaplan, *J Biomed Mater Res B Appl Biomater*, 2008, **87**, 264-285.
28. D. P. Knight, L. Nash, X. W. Hu, J. Haffegee and M. W. Ho, *Journal of Biomedical Materials Research*, 2015, **41**, 185-191.
29. W. G. C. and K. M. K., *Biochemical Journal*, 1960, **75**, 588-598.
30. A. O. Brightman, B. P. Rajwa, J. E. Sturgis, M. E. McCallister, J. P. Robinson and S. L. Voytik-Harbin, *Biopolymers*, 2000, **54**, 222-234.
31. S. T. K. a. S. L. Voytik-Harbin, *Matrix Biology*, 2009, **28**, 336–346.
32. J. L. Puetzer and L. J. Bonassar, *Acta Biomaterialia*, 2013, **9**, 7787–7795.
33. E. Bell, B. Ivarsson and C. Merrill, *Proc Natl Acad Sci U S A*, 1979, **76**, 1274-1278.
34. K. R. Johnson, J. L. Leight and V. M. Weaver, *Methods Cell Biol*, 2007, **83**, 547-583.
35. A. Nyga, M. Loizidou, M. Emberton and U. Cheema, *Acta Biomater*, 2013, **9**, 7917-7926.
36. U. Cheema and R. Brown, *Adv Wound Care (New Rochelle) , 2 (4) 176 - 184. (2013)*, 2013, **2**, 176-184.
37. M. Marotta and G. Martino, *Anal Biochem*, 1985, **150**, 86-90.
38. , ASTM Internation, West Conshohocken, PA, Editon edn., 2014.
39. S. L. Voytik-Harbin, B. Rajwa and J. P. Robinson, *Methods Cell Biol*, 2001, **63**, 583-597.
40. A. O. B. Sherry L. Voytik-Harbin, B.Z. Waisner,J. Paul Robinson,C.H. Lamar, *Tissue Eng.*, 1998, **4**, 157-174.
41. J. M. Wallace, Q. Chen, M. Fang, B. Erickson, B. G. Orr and M. M. Banaszak Holl, *Langmuir*, 2010, **26**, 7349-7354.
42. D. T. Woodley, M. Yamauchi, K. C. Wynn, G. Mechanic and R. A. Briggaman, *J Invest Dermatol*, 1991, **97**, 580-585.
43. K. Gelse, E. Poschl and T. Aigner, *Adv Drug Deliv Rev*, 2003, **55**, 1531-1546.
44. W. Friess, *Eur J Pharm Biopharm*, 1998, **45**, 113-136.
45. D. P. Speer, M. Chvapil, C. D. Eskelson and J. Ulreich, *Journal of Biomedical Materials Research*, 2015, **14**, 753-764.
46. P. Angele, J. Abke, R. Kujat, H. Faltermeier, D. Schumann, M. Nerlich, B. Kinner, C. Englert, Z. Ruszczak, R. Mehrl and R. Mueller, *Biomaterials*, 2004, **25**, 2831–2841.

47. I. V. Yannas, J. F. Burke, C. Huang and P. L. Gordon, *J Biomed Mater Res*, 1975, **9**, 623-628.
48. J. M. Gimble and F. Guilak, *http://dx.doi.org/10.1080/14653240310003026*, 2009, **5**, 362-369.
49. F. Guilak, K. E. Lott, H. A. Awad, Q. Cao, K. C. Hicok, B. Fermor and J. M. Gimble, *Journal of Cellular Physiology*, 2015, **206**, 229-237.
50. P. Carinci, M. Bodo, R. Evangelisti and E. Becchetti, *Ital J Anat Embryol*, 1995, **100 Suppl 1**, 65-74.
51. S. Rhee and F. Grinnell, *Adv Drug Deliv Rev*, 2007, **59**, 1299-1305.
52. A. M. Pizzo, K. Kokini, L. C. Vaughn, B. Z. Waisner and S. L. Voytik-Harbin, *J Appl Physiol (1985)*, 2005, **98**, 1909-1921.
53. *Advanced Drug Delivery Reviews*, 2003, **55**, 1531–1546.
54. S. M. Sweeney, J. P. Orgel, A. Fertala, J. D. McAuliffe, K. R. Turner, G. A. D. Lullo, S. Chen, O. Antipova, S. Perumal, L. Ala-Kokko, A. Forlino, W. A. Cabral, A. M. Barnes, J. C. Marini and J. D. S. Antonio, *Journal of Biological Chemistry*, 2008, **283**, 21187-21197.
55. *Mechanisms of Ageing and Development*, 1998, **106**, 1–56.
56. O. Singh, S. S. Gupta, M. Soni, S. Moses, S. Shukla and R. K. Mathur, *J Cutan Aesthet Surg*, 2011, **4**, 12-16.
57. K. G. Cornwell, A. Landsman and K. S. James, *Clinics in Podiatric Medicine and Surgery*, 2009, **26**, 507-523.
58. M. McClure, G. D. Duncan, G. V. Born and F. Robicsek, *Haemostasis*, 1987, **17**, 349-352.
59. C. Neu and G. Genin, *Handbook of Imaging in Biological Mechanics*, CRC Press, 2014.
60. D. A. F. F. Ysabel M. Bello, William H. Eaglstein, *American Journal of Clinical Dermatology*, 2012, **2**, 305-313.
61. W. R. Wagner, J. M. Pachence, J. Ristich and P. C. Johnson, *J Surg Res*, 1996, **66**, 100-108.
62. ASTM, Editon edn., 1986.
63. D. O. Freytes, R. S. Tullius and S. F. Badylak, *Journal of Biomedical Materials Research Part B: Applied Biomaterials*, 2015, **78B**, 327-333.
64. G. Vazquez, E. Alvarez and J. M. Navaza, 2002, **40**, 611-614.
65. S. V. Madihally and H. W. Matthew, *Biomaterials*, 1999, **20**, 1133-1142.
66. R. Roeder, J. Wolfe, N. Lianakis, T. Hinson, L. A. Geddes and J. Obermiller, *Journal of Biomedical Materials Research*, 2015, **47**, 65-70.
67. K. Billiar, J. Murray, G. Abraham and N. Bachrach, *Journal of Biomedical Materials Research*, 2015, **56**, 101-108.
68. T. M. F. Donna Schulz Torres, Ioannis V Yannas, Myron Spector, *Biomaterials*, 2000, **21**, 1607–1619.
69. *Advanced Drug Delivery Reviews*, 2003, **55**, 1613–1629.